Int. J. Nonlinear Anal. Appl.
10 (2019) Special Issue (Nonlinear Analysis in Engineering and Sciences), 1-11
ISSN: 2008-6822 (electronic)
https://dx.doi.org/10.22075/IJNAA.2019.4392

A New Semi-Active Magnetorheological Engine Mounts for Improving Vehicle Ride Comfort using Sliding Mode Controller

J. Marzbanrad*[a], S. S. Hosseini[b]

[a] Faculty at School of Automotive Engineering, Iran University of Science and Technology, Tehran, Iran,
[b] PhD Student at School of Automotive Engineering, Iran University of Science and Technology, Tehran, Iran

Abstract

In this paper, a new semi-active magnetorheological (MR) engine mount in half car model is proposed for improving ride comfort. Such a model uses a dynamic sliding mode controller. It operates as a controller system for controlling the magnetic field strength of the engine mount coil. Controlling the magnetic field strength leads to change the magnetorheological liquid properties and thereby the generated force by the liquid. This controller system is simulated and the obtained numerical results are analyzed. It is shown that such a controller has the own great role in improving vehicle ride comfort in such a way that it can remove 60% of the engine's vibration amplitude in the worst case as well as the its vibration frequency is tended toward zero. Finally, 25% of the total vibration transmitted from suspension system to vehicle body is reduced. It is found that using this controller, the undesirable vibrations imposed on the passengers can be diminished despite uncertainty of the load in the model.

Keywords: Magnetorheological engine mount, Dynamic sliding mode, half car model.

1. Introduction

Since passenger convenience is important in the vehicle controlling, the engine mount can be used for reducing the undesirable vibrations imposed on the passengers due to motor misalignment and unevenness of the road. These vibrations are directly perceived by the passengers if they are not attenuated properly [1]. The road-induced vibration and engine one at idling have typically frequencies below 50Hz (suppose Mode 1: high-amplitude and low-frequency), while the amplitude of the engine

*Corresponding author
Email address: marzban@iust.ac.ir, seyedsalman.hosseini@gmail.com (J. Marzbanrad*[a], S. S. Hosseini[b])

Received: June 2019 *Revised:* September 2019

oscillation is generally less than 0.3mm and includes the frequencies in the range of 50 to 200Hz (suppose Mode 2: low-amplitude and high-frequency). These distinct vibration modes have been reported in [2]. Also, in [3, 4] has been shown that for the best isolation between the aforementioned modes, the engine mount should have high and low damping properties in low- and high-frequency excitations, respectively. To this end, a single degree of freedom (DOF) model of a suspension system has been proposed in [5] which uses a semi-active controller for isolating the base excitations to the vehicle body. In addition, using a semi-active tunable dynamic absorber with a two DOF model leads to suppress the vibrations of the structure more effectively [6].

To applying a semi active controller, one can use the magneto-rheological (MR) fluids in the isolation of vehicle vibrations by using it in engine mounts and suspension systems with the varying their parameters [7, 8]. Such a fluid can maximize the variability of damping and stiffness of Hydraulic Engine Mounts (HEMs). It flows between the two chambers surrounded with electromagnets. The viscosity of this fluid, and hence the critical frequency of the damper dynamically varies in order to provide satisfactorily controlling for different road conditions.

To improve vehicle ride quality, it has been used both passive and active engine mounts as well as the different vehicle models (quarter/half/full) in the literature. As mentioned above, utilizing smart MR fluid leads to semi-active engine mounts like that the reported work in [9]. In the same paper, it has been demonstrated that Sliding Mode Controller (SMC) is one of the best candidates for attenuation of the system uncertainties and its distributions. SMC, which is an approach for the design of a robust controller with the respect of uncertainties and disturbances, use a high-frequency signal to enforce the system trajectories onto a surface, and remain in this surface after a finite time [10]. In [11], an SMC using electrorheological smart liquid dampers has been designed for the suspension system. In addition, a full vehicle model has been used that includes four independent semi-active dampers in the hardware-in–the–loop (HIL) simulation. The obtained results in the same work have been compared with those achieved by using a passive damper. A semi-active controller based upon the inverse model and sliding mode control strategies has been reported in [12] for the quarter-vehicle suspension with the MR damper for ride comfort and handling safety performances. In [13], a semi-active controller for independent control of the four MR suspension systems in the 7-degree of freedom (DOF) full-vehicle has been reported. In these mentioned works, the vibration of suspension system has been examined. The combination of both adaptive fuzzy sliding mode and a controller has been used in [14] for vibration control of vehicle's seat with the help of magneto-rheological damper. Using such a controller leads to improving vehicle stability, enhancing its robustness in system's uncertainties, and decreasing the vehicle seat acceleration with a factor of 30%. In order to attenuate Macpherson strut type suspension system, a controller based on an adaptive fuzzy sliding mode has been proposed in [15]. By examining the different frequency responses of the system in the random road in the same work, it has been shown that the described controlling model has a good performance near the resonance neighbors. The main drawback of SMCs is the chattering, i.e. vibrations with high-frequency and low amplitudes leads to waste the actuators energy and damage them. One of the methods for chattering elimination is the Dynamic Sliding Mode Controller (DSMC), which has been presented [10]. DSMC includes an integrator (low pass filter) placed be-fore the input control signal for removing the high frequency switching. However, it is desired to use DSMC for elimination of high-frequency engine vibration. To do so, choosing a vehicle model is required at the first step.

In this paper, the half car model is utilized which is presented in [16] as a vehicle one of our approach in which a comparative study is done to investigate some benefits and deficiencies of the dynamic sliding mode controller in respect to the semi-active system with MR damper. As a result, this system has capability in removing 60% of the engine's vibration amplitude and its vibration

frequency is diminished. In addition, the total vibration transmitted from suspension system to vehicle body is reduced by a factor of 1/4.

2. SUSPENSION SYSTEM

The vehicle suspension models can be generally divided into three types namely: quarter-car, half-car and full-car models [17]. In this study, the half-car suspension model is used. The half-car model is based on the interaction between the quarter car body and the single wheel. The motion of the half-car model is the interactions between the car body and the wheel and also between both ends of the car body. The first interaction in the half-car model causes the vertical motion and the second one produces an angular motion [16]. The details of the model and its formulation are studied in the following.

a. HALF-CAR MODEL

A sketch of the half-car model is shown in figure 1. The model has five degrees of freedom, including the vertical motions for unsprung masses of the front and rear wheels, motions of the sprung mass including heave and pitch and vertical motion of the engine. The governing equation of motion for the chassis is [16]:

$$I\ddot{\theta} + F_f a - F_r b = 0 \tag{2.1}$$
$$m_f \ddot{y}_f + K_{tf}(y_f - h_f) - F_y = 0 \tag{2.2}$$
$$m_r \ddot{y}_r + K_{tr}(y_r - h_r) - F_r = 0 \tag{2.3}$$
$$M\dot{y}_c + F_f + F_r - F_{mount} = 0 \tag{2.4}$$

in which I is the mass moment inertia of the vehicle body with respect to center of gravity, M is the sprung mass of the vehicle body, m_f and m_r are the sprung masses, y_c is the absolute displacement of the CG of the vehicle body (sprung mass), y_f and y_r represent the unsprang mass displacements, is the pitch, k_f and k_r denote the passive suspension stiffness's, c_f and c_r are passive suspension damping coefficients, k_{tf} and k_{tr} represent the tire stiffness's, h_r and h_f are the random road excitations, f_{mount} is the magneto-rheological engine mount force, F_r and F_f denote to suspension system forces exerted on the sprung mass and can be written as:

$$F_f = K_f(y_c - a\theta - y_f) + C_f(\dot{y}_c - a\dot{\theta} - \dot{y}_f) = 0 \tag{2.5}$$
$$F_r = K_r(y_c - b\theta - y_r) + C_r(\dot{y}_c - b\dot{\theta} - \dot{y}_r) = 0 \tag{2.6}$$

b. ENGINE MOUNT MODEL

In this model, MR damper plays the role of a semi-active component in which the damping force is adjusted via changing the applied magnetic field. MR resistive force is denoted by f_{MR}. The equation of motion for the mount can be given as [7]:

$$m_e\ddot{y}_e + K_p(y_e - y_c) + C_p(\dot{y}_e - \dot{y}_c) = f_e - f_{MR} \tag{2.7}$$

In which m_e is the engine displacement, y_e and $\dot{y_e}^{\cdot}$ denote engine displacement and velocity respectively, K_p and K_p represent the passive stiffness and damping coefficients, respectively. In equation (2.7), f_e, is the engine's unbalanced excitation. In a vehicle engine, the dynamic forces are created by various sources such as moving components in the crank mechanism, together with the cylinder

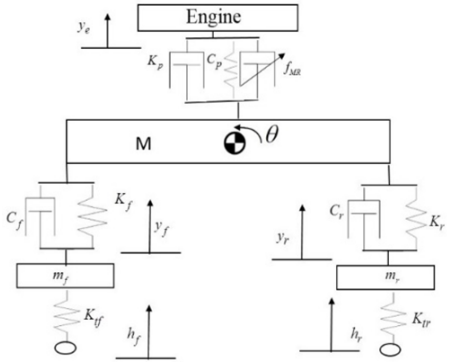

Figure 1: Semi-active engine-mount- half-car model with magnetorheological engine mount

pressure, etc. These harmonic forces are the main dynamic excitation sources in a combustion engine [18]. Therefore, fe, without loss of generality, can be given as follows [6]:

$$f_e = F_e e^{i\omega t} = m_e e \omega^2 e^{i\omega t} \tag{2.8}$$

In figure 2, the engine vibration (f_e / m_e) is depicted. As can be seen in this figure, the vibrations of the engine can be roughly modelled using the relation (2.8). In addition, in equation (2.7), the

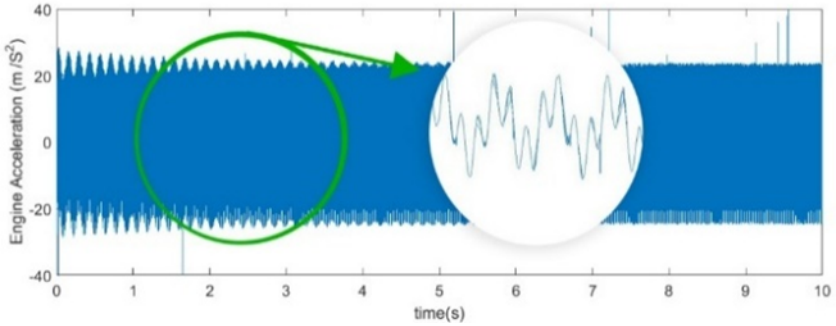

Figure 2: Engine Vibrations

MR damping force (f_{MR}) can be expressed as [7]:

$$f_{MR} = f_{yield} \frac{\dot{y}_e}{|\dot{y}_e|} \tag{2.9}$$

Where f_{yield} is diminished in the absence of the magnetic field. This force depends on fluid properties and MR damper geometry. In this study, the flow (valve) mode type of MR damper is chosen. The pressure drops created in this mode is the sum of the viscous (pure rheological) components [19]:

$$\Delta P = \Delta P_\eta + \Delta P_\tau(H) = \frac{12\eta Q L}{b h^3} + \frac{3\tau_y(H) L}{h} \tag{2.10}$$

$$Q = A_p \vartheta = \frac{\pi}{4}(D^2 - d^2)\vartheta \tag{2.11}$$

$$f_{yield} = \frac{3\tau_y(H) L \pi}{4h}(D^2 - d^2) \Longrightarrow \tau_y(H) = \frac{4h f_{yield}}{L\pi(D^2 - d^2)} \tag{2.12}$$

The fluid used for simulation is MRF-122EG made by LORD Company. Fluid's yield stress and magnetic flux density related to magnetic field intensity are displays in figure 3.

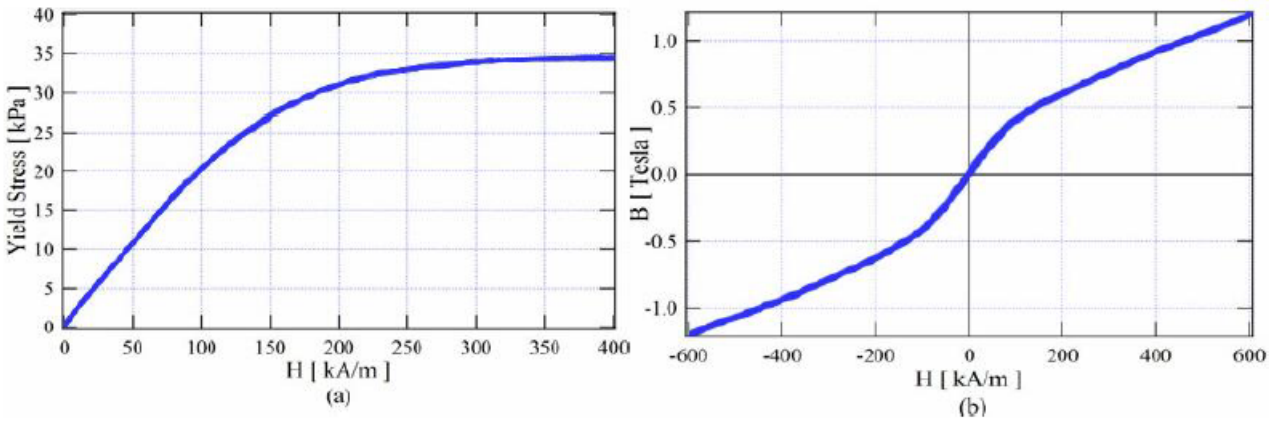

Figure 3: Characteristic curves of MRF-122EG related to magnetic field intensity (H), a) Yield stress b) magnetic flux density

With regard to coil properties, it can produce the limited magnetic flux density and magnetic field intensity, so the only operating area of the coil is regarded. By using the curve fitting method in the operating area, the B-H-Yield stress surface can be obtained. The coil current related to

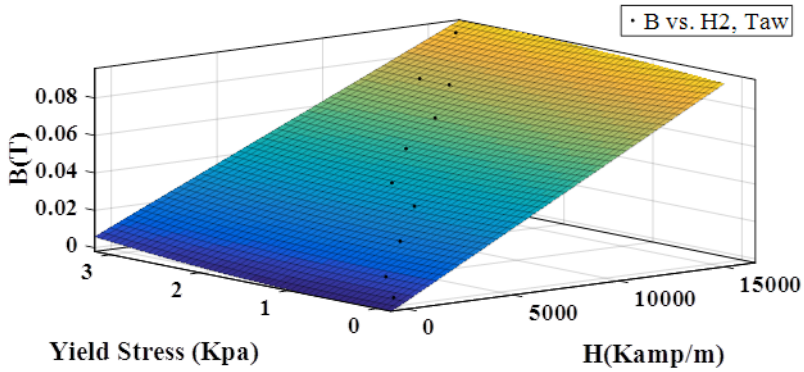

Figure 4: Characteristic curves of MRF-122EG related to magnetic field intensity (H), a) Yield stress b) magnetic flux density

magnetic flux density is obtained as:

$$B = \frac{\mu N I}{2\pi R} \Longrightarrow I_{controller} = B = \frac{2\pi R B}{\mu N} \tag{2.13}$$

in which N is the number of coils, I am the coil current and because of technical restrictions the maximum coil current is set to 3 amps and R is the coil mean radius and μ is the fluid permeability constant. By using the surface in the figure 4 the desired magnetic flux density can be computed. With regard to equation(2.13), the controller current is calculated. In the next section, the controller design is described.

3. DYNAMIC SLIDING MODE CONTROLLER

In this section, controller design is described. The goal of the controller design is passenger's comfort. A dynamic sliding controller is designed for removing engine disturbances.

a. DESIGN OF SLIDING MODE CONTROLLER

As stated in equation (2.4) the system input is the force produced by the engine mount (f_{mount}). This force should be determined such that the center of mass displacement, velocity and acceleration tends to zero:

The desired sliding surface is:

$$x_1 = y_c, \qquad x_1 = \dot{y}_c, \qquad x_1 = \ddot{y}_c \tag{3.1}$$

$$s = \lambda_1 x_1 + \lambda_2 x_2 + \lambda_3 x_3 \tag{3.2}$$

The coefficients of equation (3.2) must be selected according to the Hurwitz conditions:

$$\lambda_3 p^2 + \lambda_2 p + \lambda_1 = 0 \tag{3.3}$$

The sliding surface derivative is:

$$\dot{S} = \lambda_1 x_2 + \lambda_2 x_1 + \lambda_3 \dot{x}_3 \tag{3.4}$$

By replacing $\ddot{y}_c$ from equation(2.4) and by factorization of x_1, x_2 and x_3:

$$\begin{aligned}
\dot{S} &= \lambda_1 x_2 + \lambda_2 (x_3) + \frac{\lambda_3}{M}(F_f + F_r - f_{mount}) \\
&= \lambda_1 x_2 + \lambda_2 (x_3) + \lambda_3 \big(K_f(x_2 + a\dot{\theta} - \dot{y}_f) + C_f(x_3 + a\ddot{\theta} - \ddot{y}_f) \\
&+ K_r(x_2 + b\dot{\theta} - \dot{y}_r) + C_r(x_3 + b\ddot{\theta} - \ddot{y}_r) - \dot{f}_{mount}\big) \\
&= (\lambda_1 + \lambda_3(K_f + K_r))x_2 + (\lambda_2 + \lambda_3(C_f + C_r))x_3) + \lambda_3(K_f(a\dot{\theta} - \dot{y}_f) \\
&+ C_f(a\ddot{\theta} - \ddot{y}) + K_r(b\dot{\theta} - \dot{y}_r) + C_r(b\ddot{\theta} - \ddot{y}_r) - \dot{f}_{mount}\big)
\end{aligned} \tag{3.5}$$

By replacing $\ddot{y}_r$, $\ddot{y}_f$ and $\dot{\theta}$ into equation(3.5), the sliding surface equation is:

$$\begin{aligned}
\dot{S} &= K_1 x_1 + K_2 x_2 + K_3 y_f + K_4 \dot{y}_4 + K_5 y_r + K_6 \dot{y}_6 + K_7 \theta \\
&+ K_8 \dot{\theta} + K_9 h_f + K_{10} h_r + K_{11} f_{mount} + K_{12} \dot{f}_{mount} + K_{13} f_{dis}
\end{aligned} \tag{3.6}$$

The coefficients can be demonstrated by:

$$K_1 = \Big(\big(\lambda_2 + \lambda_3(C_f + C_r)\big)(K_f + K_r)\Big) - \lambda_3\left(\frac{C_f K_f}{m_f} + \frac{C_r K_r}{m_r} + \frac{(C_r b - C_f a)(-K_f a + K_r b}{I}\right)$$

$$K_2 = \left(\lambda_1 + \lambda_3(K_f + K_r) + \big(\lambda_2 + \lambda_3(C_f + C_r)\big)(C_f + C_r) - \lambda_3\left(\frac{C_f^2}{m_f} + \frac{C_r^2}{m_r} - \frac{(C_r b - C_f a)^2}{I}\right)\right)$$

$$K_3 = \left(\lambda_3\left(\frac{C_f(K_f - K_{tf})}{m_f} - \frac{(C_r b - C_f a)K_f a}{I}\right) + \big(\lambda_2 + \lambda_3(C_f + C_r)\big)(-K_f)\right)$$

$$K_4 = \left(\big(\lambda_2 + \lambda_3(C_f + C_r)\big)(-C_f) - (\lambda_3 K_f) - \lambda_3\left(-\frac{C_f^2}{m_f} - \frac{(C_r b - C_f a)C_f a}{I}\right)\right)$$

$$K_5 = \left(\big(\lambda_2 + \lambda_3(C_f + C_r)\big)(-K_r) + \lambda_3\left(\frac{C_r(K_r - K_{tf})}{m_r} - \frac{(C_r b - C_r a)K_r b}{I}\right)\right)$$

$$K_6 = \left(\big(\lambda_2 + \lambda_3(C_f + C_r)\big)(-C_r) - (\lambda_3 K_r) + \lambda_3\left(\frac{(C_r b - C_f a)C_r b}{I} + \frac{C_r^2}{m_r}\right)\right) \tag{3.7}$$

$$K_7 = \left(\big(\lambda_2 + \lambda_3(C_f + C_r)\big)(K_f a - K_r b) - \lambda_3 \left(\frac{C_f K_f a}{m_f} - \frac{C_r K_r b}{m_r} + \frac{(C_r b - C_f a)(-K_f a^2 - K_r b^2}{I} \right) \right.$$

$$K_8 = \big(\lambda_2 + \lambda_3(C_f + C_r)\big)(C_f a - C_r b) + \lambda_3(K_f a + K_r b) - \lambda_3 \left(\left(\frac{C_f^2 a}{m_r} + \frac{C_r^2 b}{m_r} \right) \right.$$
$$\left. + \frac{(C_r b - C_f a)}{I}(-C_f a^2 - C_r b^2) \right)$$

$$K_9 = -\lambda_3 \frac{C_f K_{tf}}{m_f}$$

$$K_{10} = -\lambda_3 \frac{C_r K_{tr}}{m_r}$$

$$K_{11} = \big(\lambda_2 + \lambda_3(C_f + C_r)\big)$$

$$K_{12} = -\lambda_3$$

By setting the surface equation to zero, desired input which can converge the outputs to zero in the finite time can be written as:

$$\dot{f_{mount}} = \frac{K_1 x_1 + K_2 x_2 + K_3 y_f + K_4 \dot{y}_4 + K_5 y_r + K_6 \dot{y}_6 + K_7 \theta + K_8 \dot{\theta} + K_9 h_f + K_{10} h_r + K_{11} f_{mount} + K_{13} f_{dis}}{K_{12}} \tag{3.8}$$

Which f_s is the upper boundary of uncertainties and equals to:

$$f_s = -\frac{1}{1-k} sat\left(\frac{s}{\varphi}\right) \tag{3.9}$$

In this equation, $\eta = |K_{13} f_{dis}| + \varepsilon$,$\varepsilon > 0$, φ is the boundary layer thickness and k is a number between 0 and 1. The sliding surface is shown in figure 5.
For simplicity, it is assumed that $h_r = h_f$ and equal to:

$$h_r = 0.05 \sin(1.5\pi t) \sin(0.15\pi t) + 0.05 \cos(0.6\pi t) \sin(0.3\pi t) \tag{3.10}$$

This assumption where the road roughness variation is insignificant along its width is correct. Figure 6 illustrates this profile asstated in the equation(3.10).

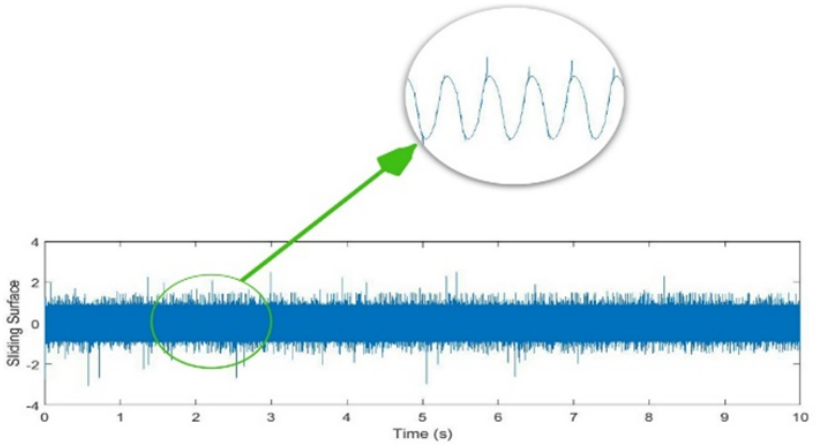

Figure 5: Sliding Surface

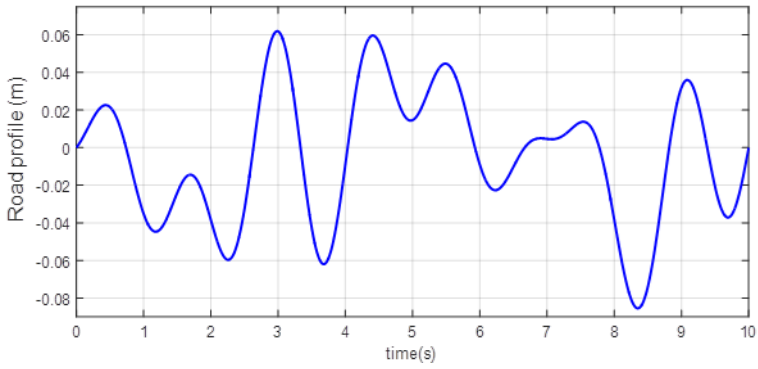

Figure 6: Road profile

b. PROOF OF STABILITY

By considering $V = \frac{1}{2}S^2$ as Liapunov function candidate:

$$\begin{aligned}\dot{V} = S\dot{S} &= S(K_1x_1 + K_2x_2 + K_3y_f + K_4\dot{y}_4 + K_5y_r + K_6\dot{y}_6 + K_7\theta \\ &+ K_8\dot{\theta} + K_9h_f + K_{10}h_r + K_{11}f_{mount} + K_{12}\dot{f}_{mount} + K_{13}f_{dis}) \\ &= SK_{13}f_{dis} - \eta f_s \leq |K_{13}f_{dis}||S| - \eta f_s \leq (|K_{13}f_{dis} - \eta)|S| \\ &\leq -\varepsilon|S| \leq 0\end{aligned} \tag{3.11}$$

Using the equation(3.11), one can obtain $t_s \leq \dfrac{|S(0)|}{\varepsilon}$ in which t_s is reaching time that expresses a finite time for the error trajectory converges to zero.

4. RESULTS AND DISCUSSIONS

In this section, the uncertainty of the chassis mass and engine mass is studied by simulation of the described model and designed controller in the previous sections. Note that in the following simulations, an Additive White Gaussian Noise (AWGN) is also taken into account for usable issues. In addition, the h_r results include the road profile (in equation (3.9)) as a system disturbance. Since the impulse response of a system is important due to achieving information of the system for all frequencies, the response of the system is simulated when an impulse is applied to the engine while the road disturbance is zero. The obtained response is depicted in Figure 7 for such an input in comparison with the one of the uncontrolled system. As shown in the same figure, by using the designed controller the chassis displacement is very negligible (<0.8 mm for $t < 0.5$ Sec.).

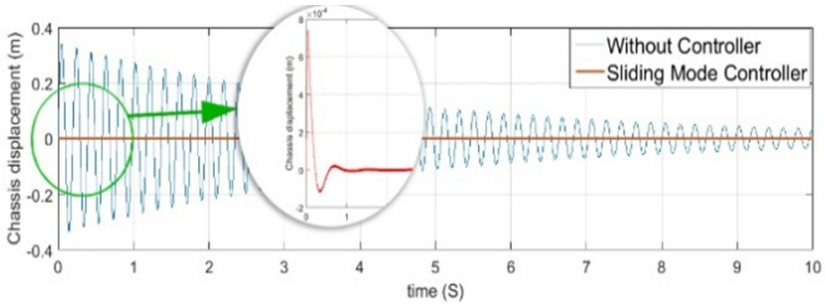

Figure 7: Chassis displacement. The result without controller is depicted for comparison.

In order to diminish the created force due to the engine vibrations, it must be produced an opposing

force by using the engine mount. This includes the resistive force produced by magnetorheological fluid and the passive one. Note that the engine force is in high frequencies; therefore, the resistance force must be in these frequencies. Figure 8 shows the total force transmitted from engine mount to vehicle body. As can be seen in the same figure, the total force fluctuates between -2500 and 2500 N. Since the passive force is yielded by intrinsic characteristic of the engine mount, it is not controllable. Thus, the former part of opposing force can be controlled by magnetorheological fluid that is affected by a magnetic field (see Figure 9). Such a magnetic field change by the designed dynamic sliding mode controller. Using the mentioned approach, the obtained opposing force when the passive part is absent, is shown in Figure 10.

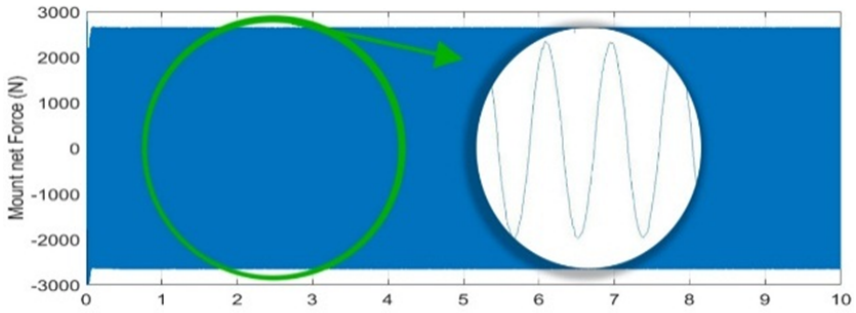

Figure 8: Applied force from engine mount to chassis

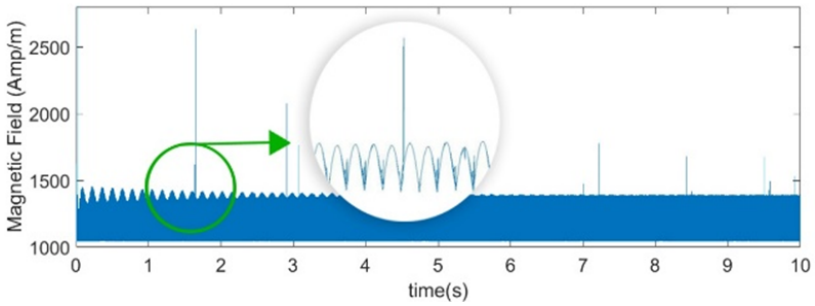

Figure 9: magnetic field intensity produced in the coil

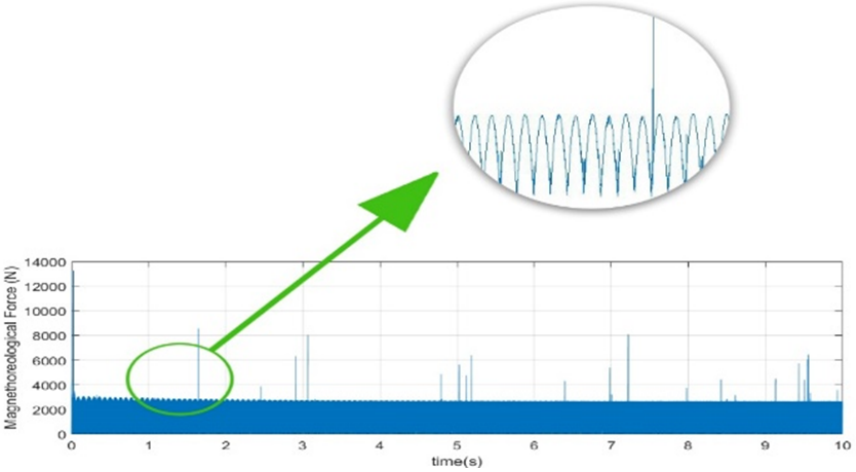

Figure 10: MRF-122EG produced force

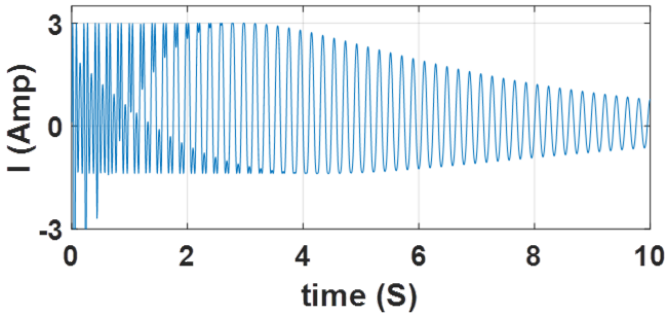

Figure 11: the coil controlled current

5. CONCLUSION

In this paper, suitable way of controlling and isolating the vibrations passing through the engine as a source of high-frequency excitation is examined. The MR damper with sliding mode controller has an optimum performance in respect to the passive engine mount one. The technical difficulties, including coil maximum dimension, current has been regarded. In addition, some uncertainties on chassis mass and engine mass and noise in road profile has been added to the system. Results show that the presented controller can overcome the uncertainties in such a way that the presented model is an efficient controller for the vehicle ride comfort. It is shown that using the controller in half-car model leads to fast converging the sliding surface and thereby very good stability.

References

[1] I. L. Ladipo, J. Fadly and W. F. Faris, Characterization of magnetorheological elastomer (MRE) engine mounts. Journal of Materials Today: Proceedings 3.2 (2016): 411-418.
[2] J. Marzbanrad, and M.A. Babalooei, Grazing bifurcations and chaos of a hydraulic engine mount. International Journal of Automotive Engineering 6.3 (2016): 2182-2190.
[3] G.N. Jazar, and F. Golnaraghi, Engine mounts for automotive applications: a survey. The Shock and Vibration Digest 34.5 (2002): 363-379.
[4] M. Zehsaz, F. Vakilitahami and A. Paykani, Investigation on the effects of stiffness and damping coefficients of the suspension system of a vehicle on the ride and handling performance. UPB Scientific Bulletin, Series D: Mechanical Engineering 76.1 (2014): 55-70.
[5] S. Baldovin and D. Baldovin, The semi-active groundhook control of SDOF systems with harmonical base excitation. UPB Scientific Bulletin, Series D: Mechanical Engineering 77.2 (2015): 27-34.
[6] M. K. Kwak, D.-H. Yang and J.-H. Shin, Active vibration control of structures using a semi-active dynamic absorber. Noise Control Engineering Journal 61.3 (2015): 287-299.
[7] S.-C. Huang, Some discussions of MR engine mount on vibration attenuation and force transmission. The 21st International Congress on Sound and Vibration. Beijing/China, 2014.
[8] A. Dobre, C. Calinoiu, T. Cojocaru-reblea and O. I. Nica, Correlation between the control current and the damping effect foe magnethorheological shock absorbers. UPB Scientific Bulletin, Series D: Mechanical Engineering 77.4 (2015): 119-130.
[9] S.-B. Choi, W. Li, M. Yu, H. Du, J. Fu and P. X. Do, State of the art of control schemes for smart systems featuring magneto-rheological materials. Journal of Smart Materials and Structures (2016): 043001.
[10] A. J. Koshkouei, K. J. Burnham and A. S. Zinober, Dynamic sliding mode control design. IEEE Proceedings-Control Theory and Applications. Stevenage, 2005. 392-396.
[11] S.-B. Choi, Y. T. Choi and D. S.-W. Park, A sliding mode control of a full-car electrorheological suspension system via hardware in-the-loop simulation. ASME Jouranl of Dynamic Systems, Measurement, and Control 121.1 (1998): 114-121.
[12] Z. Hailong, E. Wang, N. Zhang, F. Min, R. Subash and C. Su, Semi-active sliding mode control of vehicle suspension with magneto-rheological damper. Chinese Journal of Mechanical Engineering 28.1 (2015): 63-75.
[13] H. Zhang, E. Wang, F. Min, R. Subash and C. Su, Skyhook-based semi-active control of full-vehicle suspension with magneto-rheological dampers. Chinese Journal of Mechanical Engineering 26.3 (2013): 498-505.

[14] D. X. Phu, S.-B. Choi, Y.-S. Lee and M.-S. Han, Vibration control of a vehicle's seat suspension featuring a magnetorheological damper based on a new adaptive fuzzy sliding-mode controller. Proceedings of the Institution of Mechanical Engineers, Part D: Journal of Automobile Engineering 230.4 (2015): 437 - 458.
[15] S. Dutta, S.-M. Choi and S.-B. Choi, A new adaptive sliding mode control for Macpherson strut suspension system with magneto-rheological damper. Journal of Intelligent Material Systems and Structures 27.20 (2016): 2795 - 2809.
[16] J. Marzbanrad, P. Poozesh and M. Damroodi, Improving vehicle ride comfort using an active and semi-active controller in a half-car model. Journal of Vibration and Control 19.9 (2013): 1357-1377.
[17] T. Ushijima and T. Dan, Nonlinear BBA for predicting vibration of vehicle with hydraulic engine mount. SAE Technical Paper Series 860550 (1986).
[18] H. Tienhaara, Guidelines to engine dynamics and vibration. Wärtsilä Corporation (2004): 20-25.
[19] E. Guglielmino, T. Sireteanu, C. W. Stammers, G. Gheorghe and M. Giuclea, Semi-active Suspension Control. London: Springer, 2008.